Nonperturbative Study of the Rearrangement Dynamics in Ion-Atom Collisions with Active Electrons on Projectile and Target

Tom Kirchner[1,*], H. J. Lüdde[2], and M. Horbatsch[3]

[1] *Institut für Theoretische Physik, TU Clausthal, Leibnizstraße 10, D-38678 Clausthal-Zellerfeld, Germany*
[2] *Institut für Theoretische Physik, Johann Wolfgang Goethe-Universität, Robert-Mayer-Straße 8, D-60054 Frankfurt, Germany*
[3] *Department of Physics and Astronomy, York University, Toronto, Ontario, Canada M3J 1P3*

PACS numbers: 34.10.+x, 34.50.Fa, 34.70.+e

* tom.kirchner@tu-clausthal.de

Abstract

Using a single-particle picture that is based on time-dependent density functional theory we analyze the He^+-Ne collision system, in which the projectile electron as well as the target electrons undergo inelastic transitions. It is shown that many experimental cross sections can be understood if the model is applied carefully and consistently. In particular, we consider (i) the problem of nonorthogonal propagated target and projectile orbitals, (ii) the antisymmetry of the many-electron wave function, and (iii) dynamical screening effects.

1 Introduction

In an ion-atom collision experiment one often encounters the situation that electrons are attached to the target and to the projectile in the initial channel. In many cases, namely if the projectile ion is highly charged its electrons are so tightly bound that they merely screen the nucleus and undergo transitions at most with very small probabilities compared to the outer electrons of the neutral target atom. From a theoretical point of view this implies that it is not necessary to deal with the projectile electrons explicitly as long as one is interested in the dynamics of the target electrons only. It is then sufficient to treat the projectile as a point charge with fixed charge state. The situation changes, however, if one considers more symmetric collision systems, in which the binding energies of the outer target and projectile electrons are comparable. In such systems, both 'kinds' of electrons are active, i.e., they can be excited, ionized or transferred to the other center in the same event. As a consequence, one can expect interesting many-electron dynamics, but at the same time it is clear that a systematic theoretical treatment is difficult.

A natural starting point in order to disentangle the complicated situation is perturbation theory. This road was first taken by Bates and Griffing in the 1950s [1], and later on elaborated by several authors. In particular, it led to the idea that projectile electron loss, i.e., electron removal from the projectile ion is mediated either by an interaction of the projectile electron with the target nucleus, which may be screened by the target electrons (screening mode), or by an interaction with one of the target electrons, which is then excited or ionized in the same event (antiscreening mode) [2]. Both processes correspond to different amplitudes in a perturbation expansion, and in fact, they can be separated experimentally, most clearly by measuring the momentum distribution of the recoil ions [3]. Very recently, it has been suggested that the isolation of the antiscreening process gives rather clean information on electron-impact ionization (e,2e) of ions which is difficult to study directly [4].

These analyses and interpretations are restricted to fast collisions, for which low-order perturbation theory is valid. If one wishes to address intermediate and low impact energies one is faced with two interrelated problems. Firstly, higher-order contributions become increasingly important and make an order-by-order analysis impracticable and a perturbation-theory based interpretation meaningless. Secondly, electron transfer processes compete with ionization and cannot be neglected even if the interest is in ionization only.

It is the goal of this contribution to show that one can nevertheless analyze and understand experimental data taken in this regime on the basis of a relatively simple model. The model is based on an effective single-particle picture and relies on a

nonperturbative description of the collision system. As will be shown below the crucial ingredient for the successful calculation of charge-changing cross sections is a careful analysis of the single-particle solutions beyond simple statistical models.
The theoretical basis and the specifications of the model are discussed in Sec. II, while selected results are presented in Sec. III for $He^+(1s)$-Ne collisions. This system has been considered before in a similar framework [5], but less sophisticated analyses of the single-particle solutions were used. A more complete comparison of the previous and the new data as well as results for other systems (e.g., He^+-Ar) will be presented in a future work. Atomic units ($\hbar = m_e = e = 1$) are used throughout.

2 Theory

Our theoretical approach to the problem at hand with N active target electrons and one active projectile electron is based on an effective single-particle description of the $(N+1)$-electron system and the semiclassical approximation of heavy-particle collisions, in which the motion of the nuclei is described by a classical (straight-line) trajectory $\boldsymbol{R}(t)$. Although the single-particle description is approximate in practice it rests on a firm foundation provided by the basic theorems of time-dependent density functional theory (TDDFT) [6, 7]. These statements can be summarized as follows: (i) The observables of a time-dependent quantum system are unique functionals of the one-particle density $n(\boldsymbol{r}, t)$; (ii) the exact density n is given as a sum of orbital densities $|\psi_j|^2$ with orbitals that satisfy time-dependent single-particle (so-called Kohn-Sham) equations; (iii) the Kohn-Sham equations are driven by a local time-dependent potential, which is again a functional of n. The form of this potential is, however, not known exactly, and has to be approximated.

2.1 Single-particle Hamiltonians and equations

In this work, we adopt a simplified viewpoint and employ different single-particle potentials for the time development of the initial target and projectile electrons. For the initial target electrons we solve

$$i\partial_t \psi_j(\mathbf{r}, t) = \hat{h}_T(t)\psi_j(\mathbf{r}, t), \qquad j = 1, \ldots, N \tag{1}$$

with

$$\hat{h}_T(t) = -\frac{1}{2}\Delta + \left(-\frac{Q_T}{r_T} + v_{\rm ee}(r_T, t)\right) + \left(-\frac{Q_P}{r_P} + v_H^P(r_P)\right). \tag{2}$$

Q_T and Q_P are the charges of the target and projectile nuclei, and r_T and r_P denote the distances of the active electron to the target and projectile centers, respectively. We choose the target center as the origin of the reference frame such that $r_P = r_P(t) = |\boldsymbol{r}_T - \boldsymbol{R}(t)|$. The interaction of a target electron with the single projectile electron is described by the electrostatic (Hartree) potential of a hydrogenlike $1s$ orbital

$$v_H^P(r_P) = \frac{1}{r_P}[1 - (1 + Q_P r_P)\exp(-2Q_P r_P)], \tag{3}$$

while the interaction with the other $(N-1)$ target electrons consists of stationary and time-dependent parts

$$\begin{aligned} v_{\rm ee}(r_T, t) &= v_{\rm ee}([n_0]; r_T) + \delta v_{\rm ee}(r_T, t) \\ &= v_H([n_0]; r_T) + v_x([n_0]; r_T) + \delta v_{\rm ee}(r_T, t). \end{aligned} \tag{4}$$

The stationary contribution $v_{\rm ee}([n_0];r_T)$ is a functional of the ground-state density n_0 of the N-electron atom. It includes accurate Hartree (H) and exchange (x) potentials obtained from the optimized potential method (OPM) of ground-state DFT [8]. The time-dependent contribution $\delta v_{\rm ee}(r_T,t)$ accounts in a global fashion for the response of the electronic cloud in the presence of the projectile. More specifically, we use the ansatz

$$\delta v_{\rm ee}(r_T,t) = \frac{-1}{N-1}\sum_{q=1}^{N}(q-1)P_q^{\rm loss}(t)\, v_{\rm ee}([n_0];r_T), \tag{5}$$

which was suggested in Ref. [9] as a global model for the increasing attraction of the target as q electrons are removed in the course of the collision with probabilities $P_q^{\rm loss}$. We call this model *target response* model and the one that is characterized by $\delta v_{\rm ee}=0$ *no response* approximation in the following.
For the initial projectile electron specified by $j\equiv N+1$ we solve

$$i\partial_t\psi_j(\mathbf{r},t) = \hat{h}_P(t)\psi_j(\mathbf{r},t), \qquad j\equiv N+1 \tag{6}$$

with

$$\hat{h}_P(t) = -\frac{1}{2}\Delta - \frac{Q_P}{r_P} + \left(-\frac{Q_T}{r_T} + v_H^T([n_0];r_T)\right) \tag{7}$$

in the projectile reference frame, where $r_T = r_T(t) = |\boldsymbol{r}_P - \boldsymbol{R}(t)|$.
Equations (1)–(7) reflect a rather direct picture of the many-electron dynamics: The target electrons experience an atomic ground-state potential, a response potential due to their partial removal from the target atom during the collision, and the time-dependent screened projectile potential of the moving $He^+(1s)$ ion. The projectile electron experiences the Coulomb potential of the He^{2+} nucleus and the time-dependent Coulomb potential of the moving target nucleus, which is *fully* screened by the N target electrons. A more symmetric model should include also a response contribution in Eq. (7) due to the removal of the target electrons, but this refinement is not considered here. Our simpler scheme has the practical advantage that the time development of target and projectile electrons is completely uncoupled and can be computed independently. Taking response effects into account not only in the target but also in the projectile Hamiltonian would couple Eqs. (1) and (6) throughout the propagation.
We have solved the (uncoupled) single-particle equations (1) and (6) by using our basis generator method (BGM) [10]. In the BGM, the time-dependent orbitals ψ_j are expanded in a pseudo basis which is constructed such that the spanned model space is dynamically adapted to the problem at hand. For the present work we have used the same basis sets as described in Ref. [5].

2.2 Analysis of the single-particle solutions

In Ref. [5] it was discussed how one can extract probabilities and cross sections for charge-changing processes from a combinatorial analysis of single-particle transition probabilities associated with ionization and electron transfer events. The most direct way to do this is the multinomial analysis, in which q-particle transitions are given as sums of all combinations of q single-electron transition probabilities multiplied by $(N+1-q)$ single-electron probabilities for not undergoing the transition of interest. This analysis corresponds to a strict independent particle model (IPM), in which the transition of one electron is not influenced by the transitions of the other electrons.

A well-known deficiency of this model is the occurrence of significant probabilities for very unlikely or completely unphysical processes such as multiple electron-transfer events that correspond to the formation of negative ions. In Ref. [11] we have suggested a modified scheme termed *products-of-binomials* analysis which eliminates the unphysical channels explicitly and redistributes the total flux over the allowed ones statistically. This ad-hoc modification can be viewed as a step beyond the strict IPM, and it has been applied in several works with some success (see, e.g., Ref. [12]). Notwithstanding this success the products-of-binomials analysis can also be criticized for several reasons: (i) it leads to a slight imperfection in the overall probability conservation; (ii) for the present problem of He^+-Ne collisions there is no unique way to account for the fact that double capture is possible when the projectile electron is removed in the same event, but is prohibited (or at least is to be regarded as an anomaly) if it remains bound; (iii) it is not based on first-principles arguments.
In the following we describe an alternative procedure which does not suffer from these defects and which represents a systematic improvement of the strict IPM. In order to establish this analysis we first note that the single-particle orbitals associated with the initial target and projectile states are normalized due to the unitarity of the single-particle equations, but lose their orthogonality during the collision, because the Hamiltonians (2) and (7) are different

$$\hat{h}_T(t) \neq \hat{h}_P(t) \quad \rightarrow \quad S_{N+1,j}(t) \equiv \langle \psi_{N+1}(t) \mid \psi_j(t) \rangle \neq 0, \quad j = 1, \ldots, N. \tag{8}$$

At high energies, where ionization dominates this is not a practical problem, as the propagated target and projectile orbitals contribute mainly in different regions of configuration space and have negligible overlap. This is no longer true at lower collision energies, where electron transfer channels are strong. For the lowest collision energy considered ($E_P = 10$ keV/amu) we found values for the absolute square of the overlap integrals in Eq. (8) of up to 0.3.
The problem of nonzero overlap integrals $S_{N+1,j}$ cannot be avoided in a simple way, but it can be taken into account in the analysis of the single-particle solutions at the asymptotic time t_f after the collision where the propagation is stopped. As we neglect correlation effects in the potentials of Eqs. (2) and (7) the total $(N+1)$-electron wave function of the collision system is given as a single determinant with a factor that ensures normalization

$$\Psi(x_1, \ldots, x_{N+1}; t) = \frac{1}{\sqrt{(1 - \sum_{j=1}^{N+1} |S_{N+1,j}(t)|^2)(N+1)!}} \begin{vmatrix} \psi_1(x_1,t) & \ldots & \psi_{N+1}(x_1,t) \\ \vdots & \ddots & \vdots \\ \psi_1(x_{N+1},t) & \ldots & \psi_{N+1}(x_{N+1},t) \end{vmatrix} \tag{9}$$

$$\langle \Psi(t) \mid \Psi(t) \rangle = 1. \tag{10}$$

In Eq. (9), x_j denotes space and spin coordinates of the jth electron. It is straightforward to show that the corresponding one-particle density n is not given as a simple sum of orbital densities, but has to be calculated according to the expression

$$n(\boldsymbol{r}, t) = \sum_{i,j=1}^{N+1} S_{ij}^{-1} \psi_j^*(\boldsymbol{r}, t) \psi_i(\boldsymbol{r}, t) \tag{11}$$

which involves matrix elements of the inverse overlap matrix.

So-called net probabilities, which correspond to average electron numbers at the target, at the projectile or in the continuum are given as integrals of the density over the corresponding regions in configuration space at $t = t_f$ [7]. As a consequence of Eq. (11) they carry also information on the overlap of orbitals. Instead of performing these integrations in r-space we use a channel representation, in which bound target, bound projectile and the continuum contributions are characterized by finite sets of single-particle states. This procedure is better adapted to the BGM. The probability, e.g., for net recoil ion production (the average charge state of the target after the collision) is then given by

$$P_{\rm net}^{\rm rec} = N - \sum_{i,j=1}^{N+1} \sum_{k=1}^{K} c_k^i S_{ij}^{-1} c_k^{j\,*}|_{t=t_f} \tag{12}$$

with single-particle amplitudes for populating the set of target states $\{|\varphi_k^T\rangle, k = 1, \ldots, K\}$

$$c_k^i = \langle \varphi_k^T \mid \psi_i \rangle|_{t=t_f}. \tag{13}$$

Not only the net quantities, but also the more detailed probabilities that correspond to charge-state correlated events are affected by the nonvanishing overlap integrals. These probabilities can be expressed as ordered sums of basic *inclusive probabilities* $P_{f_1,\ldots,f_q}$ of finding $q < N+1$ electrons in specific states labeled by $f_1, \ldots, f_q$ while nothing is known about the final states of the other electrons [13]. One can show that the inclusive probabilities $P_{f_1,\ldots,f_q}$ can be expressed as $q \times q$ determinants of the one-particle density matrix γ^1

$$P_{f_1,\ldots,f_q} = \det(\langle f_1|\hat{\gamma}^1|f_1\rangle \cdots \langle f_q|\hat{\gamma}^1|f_q\rangle) \tag{14}$$

that has the form [cf. Eq. (11)]

$$\hat{\gamma}^1 = \sum_{i,j}^{N+1} |\psi_i\rangle S_{ij}^{-1} \langle \psi_j|. \tag{15}$$

The determinantal structure of the inclusive probabilities reflects the antisymmetry of the $(N+1)$-electron wave function, i.e., the Pauli principle. The only difference of this procedure compared to inclusive analyses that we have employed in previous works (see, e.g., Refs. [5, 11]) is Eq. (15) for the one-particle density matrix that involves elements of the inverse overlap matrix. If

$$S_{ij} = \delta_{ij} \quad i, j = 1, \ldots, N+1 \tag{16}$$

the previous schemes are readily recovered.

3 Results and Discussion

Comparing results obtained from the expressions (12) and (14) with results of the strict IPM sheds light on the role of the nonorthogonality of orbitals and the antisymmetry of the total $(N+1)$-electron wave function. We begin the discussion of these effects by considering the cross section for net recoil ion production, which is directly calculated by integration of Eq. (12) over the impact parameter and does

not bear information on the antisymmetry of the many-electron state. In Fig. 1 we compare three sets of calculations with experimental data: (i) results obtained in the no-response approximation and without taking the nonorthogonality of orbitals into account (i.e., we *assume* that $S_{N+1,j}(t_f) = 0$); (ii) results in the no-response approximation that do account for the nonorthogonality; (iii) results obtained by including the target response potential (5) in the Hamiltonian (2) and taking the nonorthogonality of orbitals into account.

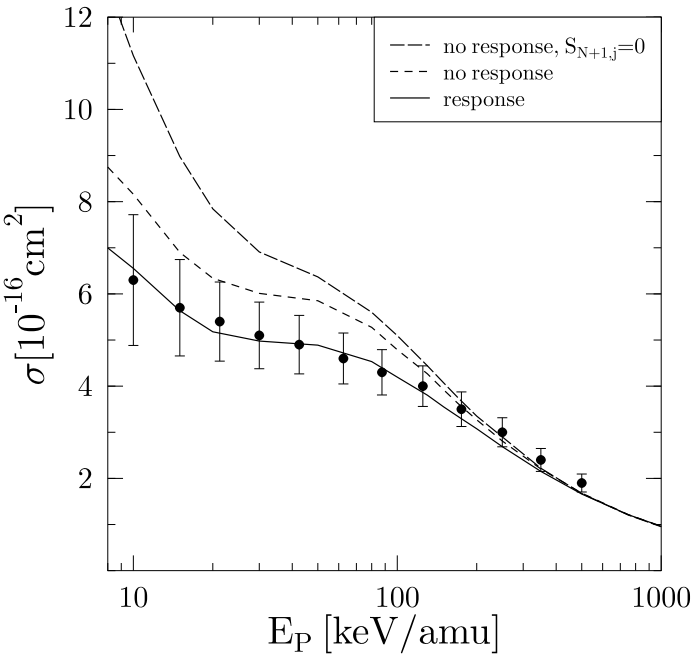

Fig. 1: Total cross section for net recoil ion production as a function of impact energy for He^+-Ne collisions. Lines: BGM results (see text for details). Symbols: experimental data from Ref. [16].

At impact energies above $E_P = 200$ keV/amu the results of all sets of calculations merge and are in good agreement with the experimenal data. This demonstrates that neither response nor nonorthogonality effects are important in fast collisions, in which ionization dominates strongly. This changes decisively towards lower impact energies where electron transfer becomes more important (cf. Fig. 3). Both effects reduce the recoil ion production cross section, and if we take both of them into account we obtain perfect agreement with experiment down to the lowest energy considered. The reduction of the cross section due to target response is obvious as the response potential (5) is attractive and increases the binding of the target electrons. The nonorthogonality effect is more subtle: the details of the calculations show that the overlap integrals (8) become appreciable when electrons are captured to the projectile with significant probabilities and occupy the same states (mainly $1s$) as the initial projectile electron. This leads to an overcounting of the population of bound projectile states which is remedied once the total probability is renormalized appropriately, i.e., if the inverse overlap matrix is not ignored but taken into account in the evaluation of $P_{\mathrm{net}}^{\mathrm{rec}}$ [Eq. (12)].

In Fig. 2 we show similar results for net free electron production, which is the sum of target and projectile ionization. In this case, the no-response approximation in conjunction with the neglect of the finite overlap integrals leads to good agreement with experiment over the entire range of impact energies displayed in the figure. However, this agreement is fortuitous as response and nonorthogonality effects are

not negligible: The consideration of the inverse overlap matrix in the net probability causes an increase of the cross section at low and intermediate impact energies. This behavior reflects the fact that the overcounting of electrons in bound projectile states is partly compensated by continuum channels. Target response counterbalances this effect and brings the data back into within the experimental error bars, except for the lowest impact energies where the theoretical cross section is still too high and appears to have a wrong slope. We expect that a more refined response model will solve this problem as response effects are obviously very important in slow collisions, but are taken into account only in a global fashion by Eq. (5).

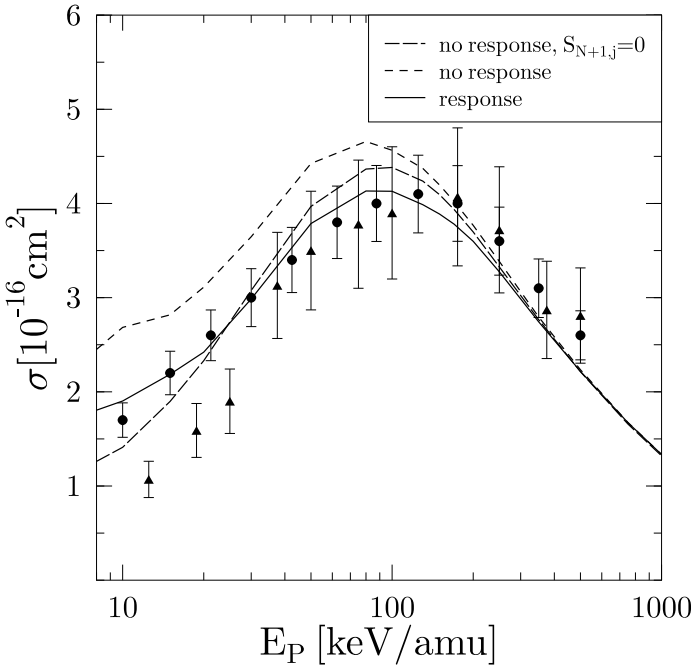

Fig. 2: Total cross section for net free electron production as a function of impact energy for He^+-Ne collisions. Lines: BGM results (see text for details). Symbols: experimental data from Ref. [16] (full circles) and Ref. [17] (full triangles).

We proceed with considering the cross sections for finding respectively two and zero electrons at the projectile after the collision, i.e., electron capture and electron loss. In Fig. 3 we show results for capture obtained from three different analyses of the single-particle solutions within the target response model: (i) the standard multinomial analysis for single capture; (ii) the same analysis, but this time single and multiple capture contributions are added; (iii) the improved analysis described in Sec. 2.2 that in contrast to the cases (i) and (ii) accounts for the antisymmetry and the finite overlap of the propagated orbitals (these results are termed 'Pauli' in the figure).
As expected, unphysical multiple capture events are strong in the standard multinomial analysis at low impact energies. Above 100 keV/amu the results of the two multinomial models merge, but they overestimate experiment by almost a factor of two up to the highest energies considered. This is a direct consequence of the neglect of the Pauli principle in the final states: As explained in closer detail in Ref. [5] both spin-up and spin-down electrons contribute to capture and are not hindered by the fact that the dominant final $He(1s^2)$ state, which is mainly formed by single capture plus elastic scattering of the initial projectile electron is a spin singlet. The problem is solved if we use our improved analysis based on inclusive probabilities. In addition, this model does not yield appreciable multiple capture cross sections at low impact

energies for the very same reason: only two electrons are allowed to populate the K shell due to the Pauli principle.

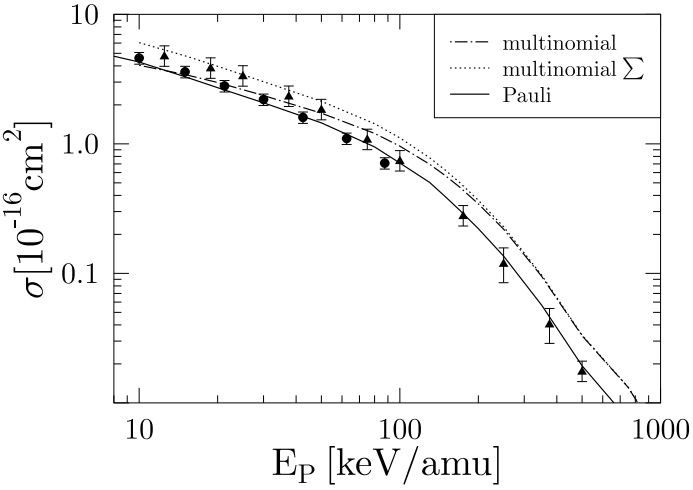

Fig. 3: Total cross section for neutralization of the projectile as a function of impact energy for He^+-Ne collisions. Lines: BGM results (see text for details). Symbols: experimental data from Ref. [16] (full circles) and Ref. [17] (full triangles).

It was also explained in Ref. [5] how the antisymmetry of the many-electron wave function can influence the electron loss channel displayed in Fig. 4 even if there is no apparent blocking of the relevant final states. Briefly, the inclusive analysis redistributes the transferred electron density from $\mathrm{Ne}(K,L)$ such that He^0 and He^{2+} formation is reduced, but He^+ formation is increased compared to the multinomial analysis. This effect is somewhat weakened by the occurrence of the finite overlap integrals [Eq. (8)] that we did not consider in Ref. [5]. Figure 4 shows that the present 'Pauli' analysis leads to a reduction of the multinomial electron loss cross section at impact energies where capture, i.e., He^0 formation is strong, but in contrast to our previous results (denoted by 'Pauli, $S_{N+1,j} = 0$') a substantial discrepancy with experiment persists. As the present analysis is clearly more consistent than the previous one from a theoretical point of view this implies that the electron loss channel is not yet understood properly at low impact energies. The next step should be a more refined treatment of response effects in order to approach the exact 'exchange-only' limit of TDDFT, in which only electron correlations are neglected, but all other effects are taken into account accurately. It remains to be seen whether one can understand the smallness of the experimental electron loss cross section below $E_P = 100$ keV/amu in this framework or whether electron correlation effects must also be considered.

Electron correlations beyond the exchange-only limit are known to play a role at higher impact energies, where the results of our different analyses coincide but somewhat underestimate experiment. In this region, the (e,2e)-like interaction of the projectile electron with one of the target electrons (antiscreening) contributes to the electron loss cross section. The contribution has been calculated in the Born approximation [14] and, very recently, in the local plasma approximation within the dielectric formalism [15], and if it is added to our results the agreement with experiment is improved.

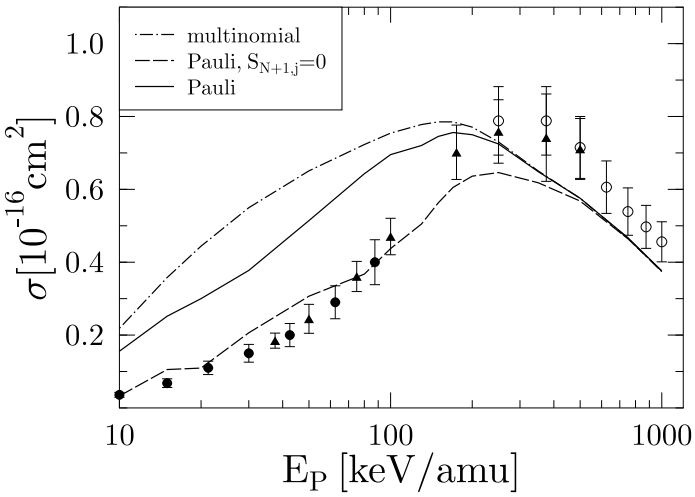

Fig. 4: Total cross section for electron loss from the projectile as a function of impact energy for He^+-Ne collisions. Lines: BGM results (see text for details). Symbols: experimental data from Ref. [16] (full circles), Ref. [17] (full triangles), and Ref. [18] (open circles).

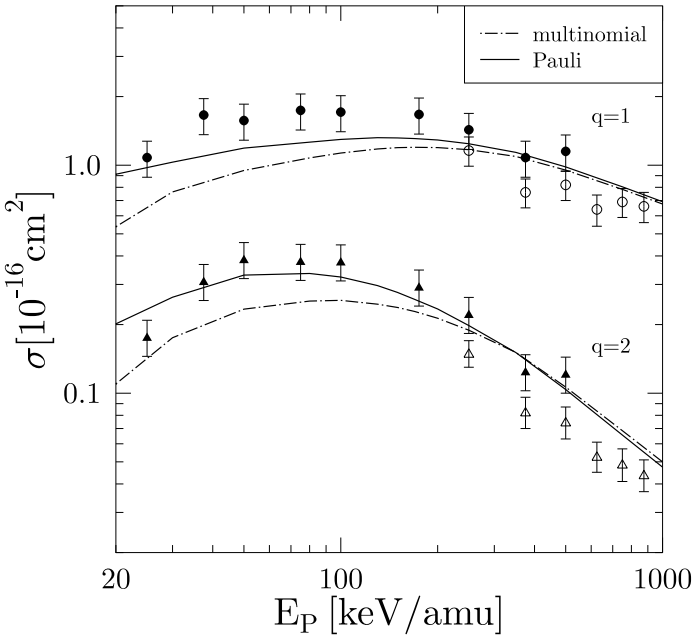

Fig. 5: Total cross section for pure single ($q = 1$) and double ($q = 2$) target ionization as a function of impact energy for He^+-Ne collisions. Lines: BGM results (see text for details). Symbols: experimental data from Ref. [17] (full symbols) and Ref. [19] (open symbols).

Finally, we show in Fig. 5 charge-state correlated cross sections for pure single and double ionization of Ne, where the projectile does not change its charge state. As discussed above (and predicted in Ref. [5]) the inclusive analysis increases these cross sections which correspond to He^+ formation compared to the multinomial results. Remarkably, rather good agreement with experiment, in particular for double ionization is obtained in this model. This demonstrates again that the antisymmetry of the many-electron wave function can affect the results significantly even if no obvious Pauli blocking is operating. The reason for this subtle effect is the interrelation and competition of different inelastic processes, in our case He^0, He^+, and He^{2+} formation in the nonperturbative regime.

4 Concluding Remarks

It was the purpose of this work to demonstrate that rather complicated many-electron dynamics in ion-atom collisions with active electrons on projectile and target centers can be understood on the basis of a single-particle picture which is sensitive to the details of the electron rearrangement processes. In particular, our results show that it is crucial to take into account the nonorthogonality of the propagated orbitals if projectile and target electrons experience different potentials. Moreover, the antisymmetry of the final many-electron wave function as well as response effects in the time-development of the system are important ingredients for a successful description of experimental data. A necessary prerequisite for this study has been the development of the basis generator method to obtain accurate solutions of the single-particle equations under discussion.

In future work, we plan to test our model also on other collision systems with active projectile and target electrons for which theoretical data is lacking. In addition, we will refine the dynamical screening model in order to approach the exact exchange-only limit of density functional theory. We believe that this will alleviate some of the remaining discrepancies with experiments and — where this is not the case — help us to pinpoint true electron correlation effects from the perspective of a well-founded and meaningful theoretical treatment.

References

[1] Bates, D.R. and Griffing, G., Proc. Phys. Soc. London Sect. A **66**, 961 (1953); **67**, 663 (1954); **68**, 90 (1955).

[2] McGuire, J.H., "Electron Correlation Dynamics in Atomic Collisions" (Cambridge University Press, Cambridge 1997), Chap. 8.

[3] Dörner, R. *et al.*, Phys. Rev. Lett. **72**, 3166 (1994); Wu, W. *et al.*, *ibid.* **72**, 3170 (1994); Phys. Rev. A **55**, 2771 (1997).

[4] Kollmus, H. *et al.*, Phys. Rev. Lett. **88**, 103202 (2002).

[5] Kirchner, T. and Horbatsch, M., Phys. Rev. A **63**, 062718 (2001).

[6] Gross, E.K.U., Dobson, J.F. and Petersilka M., in "Topics in Current Chemistry", edited by Nalewajski, R.F. (Springer, Heidelberg 1996), Vol. 181, p. 81.

[7] Lüdde, H.J., in "Many-Particle Quantum Dynamics in Atomic and Molecular Fragmentation", edited by Ullrich, J. and Shevelko, V.P. (Springer, Berlin 2003), Chap. 12.

[8] Engel, E. and Vosko, S.H., Phys. Rev. A **47**, 2800 (1993).

[9] Kirchner, T., Horbatsch, M., Lüdde, H.J. and Dreizler, R.M., Phys. Rev. A **62**, 042704 (2000).

[10] Lüdde, H.J., Henne, A., Kirchner, T. and Dreizler, R.M., J. Phys. B **29**, 4423 (1996); Kroneisen, O.J., Lüdde, H.J., Kirchner, T. and Dreizler, R.M., J. Phys. A **32**, 2141 (1999).

[11] Kirchner, T., Lüdde, H.J., Horbatsch, M. and Dreizler, R.M., Phys. Rev. A **61**, 052710 (2000).

[12] Lüdde, H.J., Kirchner, T. and Horbatsch, M. in "Photonic, Electronic, and Atomic Collisions", edited by Burgdörfer, J., Cohen, J., Datz, S. and Vane, C.R. (Rinton Press, Princeton 2002) p. 708.

[13] Lüdde, H.J. and Dreizler, R.M., J. Phys. B **18**, 107 (1985).

[14] Montenegro, E.C. and Meyerhof, W.E., Phys. Rev. A **43**, 2289 (1991).

[15] Montanari, C.C., Miraglia, J.E. and Arista, N.R., Phys. Rev. A **67**, 062702 (2003).

[16] Rudd, M.E., Goffe, T.V., Itoh, A. and DuBois, R.D., Phys. Rev. A **32**, 829 (1985).

[17] DuBois, R.D., Phys. Rev. A **39**, 4440 (1989).

[18] Sant'Anna, M.M., Melo, W.S., Santos, A.C.F., Sigaud, G.M. and Montenegro, E.C., Nucl. Instrum. Methods Phys. Res B **99**, 46 (1995).

[19] Santos, A.C.F., Melo, W.S., Sant'Anna, M.M., Sigaud, G.M. and Montenegro, E.C., Phys. Rev. A **63**, 062717 (2001).